Free-running emerald laser pumped by laser diode

Zhenqiang Chen (陈振强)[1] and Ge Zhang (张 戈)[2]

[1]*Institute of Optoelectronic Engineering, Jinan University, Guangzhou 510632*

[2]*Fujian Institute of Research on the Structure of Matter, Chinese Academy of Sciences, Fuzhou 350002*

Received June 14, 2006

Free-running emerald laser pumped by 660-nm laser diode (LD) was reported. Free-running output power of 24 mW has been obtained with overall efficiency of 1.4% and slope efficiency of 11.9% when the LD incident power was 2.56 W. The laser threshold value of emerald crystal was estimated to be 0.7 W.

OCIS codes: 140.3580, 140.3070.

Emerald (Cr^{3+}:$Be_3Al_2Si_6O_{18}$) is a negative uniaxial crystal and belongs to the hexagonal system with a space group D_{6h}^2 (P6/mcc). Owing to transition of the Cr^{3+} ion, the emerald crystal is a more efficient wideband tunable laser medium among many Cr^{3+}-doped lasing media. Compared with the alexandrite, the emerald has a more complex crystal structure and a weaker crystal field. The emission cross-section of the emerald is approximately four times larger than that of the alexandrite. Its melting point is 1470 °C, lower than that of alexandrite (1870 °C). The thermal conductivity of the emerald is 0.04 W/cm·deg, being nearly six times less than that of the alexandrite[1]. Since 1982, the emerald lasers have been achieved running with pumping by flash lamp, shot-pulse laser generated by a Nd:YAG pumped $Ba(NO_3)_2$ Raman laser, an argon laser, and a krypton continuous wave (CW) laser[1−7]. Lai[6] reported that the laser output-slope efficiency of 64% was achieved with the use of higher optical quality emerald crystal and high efficient resonator. But nowadays, the emerald lasers have been only marginally applied due to producing adequate size crystal with difficulty, limitation of growth method, poor optical quality, and intense thermal effect. In the course of our studies on the growth conditions of emerald crystals in a new hydrothermal solution[8−10], the quality of emerald crystals has been improved from gem quality to optical quality. With the development of high power laser diode (LD) and the improvement of emerald quality, the LD pumping emerald laser is essential to be studied. In this paper, we report an emerald free-running laser at 731-nm wavelength pumped by 660-nm LD. To our knowledge, this is the first letter about the emerald laser pumped by LD.

We had reported the optical spectra of emerald crystal[11]. The polarized absorption spectra of Cr^{3+}:$Be_3Al_2(SiO_3)_6$ crystal are shown in Fig. 1. The dominant features are two broad bands with peaks at 598 (σ-polarization), 646 (π-polarization), and 430 (σ-polarization), 416 nm (π-polarization) corresponding to transition from the $^4A_2$ ground state to the $^4T_2$ and $^4T_1$ excited states of the Cr^{3+} ion in octahedral coordination splitted by symmetry distortion. The narrow absorption lines (R-line) at 684 nm stem from the spin-forbidden $^4A_2 \rightarrow {}^2E$ transition in the emerald crystal. The hollow near 640-nm superposed absorption band of the $^4A_2 \rightarrow {}^4T_2$ is a characteristic of low field crystal, which can be interpreted in terms of an interaction between the sharp intra-t_2^3-levels (^2E, $^2T_1$ and $^2T_2$) and the vibrationally broadened $t_2^2e(^4T_1)$ quasi-continuum, resulting in Fano-type anti-resonance[11,12].

The photoluminescence spectrum of emerald was measured at 300 K by FLS-920 fluorescence spectra meter. As shown in Fig. 2, the most noticeable component of photoluminescence is a clear wideband peak at 731 nm in the range of 670—840 nm, corresponding to the $^4T_2 \rightarrow {}^4A_2$ transition. The R-line transition ($^2E \rightarrow {}^4A_2$) at 684 nm is not so strong as in alexandrite because of the smaller energy gap (400 cm^{-1}) between the levels ^2E and $^4A_2$. At room temperature, the lifetime of the excited state of Cr^{3+} was measured to be 63.54 μs, which is slightly smaller than the value (65 μs) reported in Ref. [1] and slightly higher than the value (45$\pm$5 μs) reported in Ref. [7].

Figure 3 shows the emerald basic plano-concave cavity,

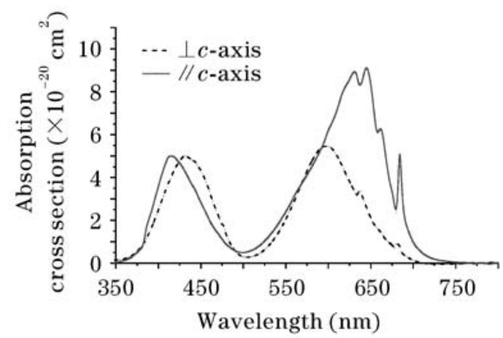

Fig. 1. Polarized absorption spectra of emerald crystal.

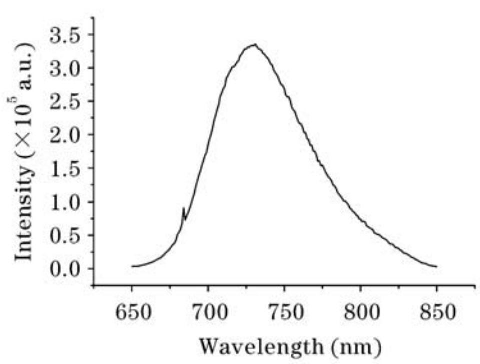

Fig. 2. Fluorescence spectrum of hydrothermal emerald.

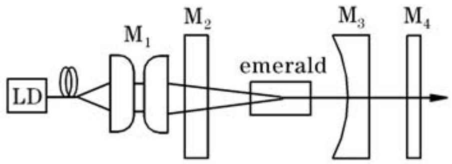

Fig. 3. Experimental setup of emerald laser.

which consisted of coupling lens system M_1, input coupling mirror M_2, output coupling mirror M_3 with curvature radius of 150 mm, and a long wave pass color filter M_4. M_2 was coated with high reflection (HR) at lasing wavelength ($R = 96.9\%$ at 731 nm) and with high transmission at the pump wavelength ($T = 93.4\%$ at 660 nm). M_3 was coated with HR in the range of 650—680 nm and partial transmitting at 731-nm wavelength ($T = 1.12\%$).

In order to investigate the output characteristics of emerald laser and obtain high gain 731-nm laser with π polarization, two emerald rods were cut according to the optical axis orientation and growth planes in crystal. The two emerald rods were 10.5- and 3.4-mm-length with cross section of 3×4 (mm) and 1.01 at.-% Cr^{3+}, pumped longitudinally by 660-nm LD respectively. Two surfaces of every emerald rod were coated with antireflection (AR).

Measuring equipment was consisted of a monochrometer, a LPE-1A laser power-meter (Physcience Optoelectronics Co., Ltd. in Beijing), and the pump source of 2.68-W 660-nm fiber-coupled LD with a core diameter of 0.8-mm and a numerical aperture of 0.22 (Hi-Tech Optoelectronics Co., Ltd.). A 56-W type monochromator (Shanghai Factory of Optical Apparatus) was used to measure the laser wavelength. The fiber output was focused into the emerald crystal and the pump spot size was about 0.80 mm.

In order to enhance the matched degree between spectral width of LD and absorbed spectrum of emerald crystal at 646 nm, the temperature of LD is controlled by a thermoelectric (TE) cooler at first and then the hot end of TE cooler is also cooled by self-circulated water with a closed-loop refrigerated recirculator. As a result, the temperature of LD is tuned to 17 °C with fluctuation less than ±0.15 °C.

Figures 4 and 5 show the free-running laser output versus input power for different emerald rods pumped by 660-nm LD in plano-concave cavity. When the LD incident power was 2.68 W (corresponding to LD output power after M_1), 2.7-mW output power at 731 nm was obtained with optical-optical conversion efficiency of 0.16% and slope efficiency of 1.76% in the length of 10.5-mm emerald rod. When the rod of 3.4-mm-length was used in the same plano-concave cavity, the largest input power at 731 nm was 23.84 mW with optical-optical conversion efficiency of 1.4% and slope efficiency of 11.9%. The full-width at half-maximum (FWHM) of 20 nm at 22-mW output power was measured. The value was lower than that of Ref. [1]. The laser threshold was about 0.7 W, which was lower than that of Refs. [1,2] and higher than that of Ref. [5].

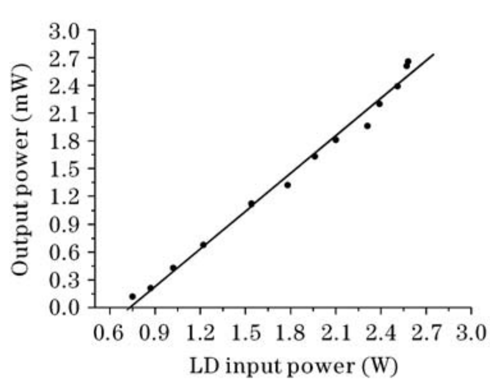

Fig. 4. Output power at 731 nm as a function of LD incident power with the rod length of 10.5 mm.

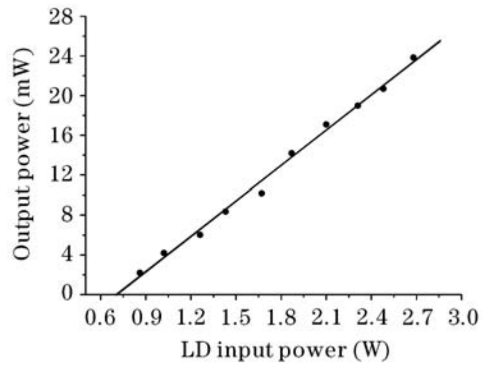

Fig. 5. Output power at 731 nm as a function of LD incident power with the rod length of 3.4 mm.

The experimental results of both emerald rods were obviously different. The scattering inclusions and the growth planes (or the growth layers) in the hydrothermal emerald were one of the key reasons which influenced the output power. Furthermore, the thermal effect was another important reason[13].

Compared with other authors' papers[4,5], the laser output power of emerald is correspondingly lower. The primary reasons were the disagreement between the wavelength of the pump source of 660 nm and the maximal absorption line of 646-nm with π polarization, the longitudinal pumping is longer than that of Refs. [1—6]. Another important reason was that the high quality coating film was difficultly gotten because of the adjacence between 660- and 731-nm wavelengths.

In summary, a 660-nm LD pumping high-stability 731-nm emerald free-running CW laser is reported in this letter. The free-running output as high as 24 mW has been obtained at 731 nm with an overall efficiency of 1.4% and a slope efficiency of 11.9% and its performances have been described.

This work was supported by the Natural Science Foundation of China (No. 60278025). We thank Prof. H. Y. Shen (Fujian Institute of Research on the Structure of Matter, CAS), associate Prof. C. H. Huang (Fujian Institute of Research on the Structure of Matter, CAS) and Prof. Y. L. Zhang (Institute of Optoelectronic Engineering, Jinan University) for their helpful discussion.
Z. Chen's e-mail address is tzqchen@jnu.edu.cn.

References

1. V. V. Antsiferov, Techn. Phys. **45,** 1085 (2000).
2. M. L Shand and J. C. Walling, IEEE J. Quantum Electron. **18,** 1829 (1982).
3. J. Buchert, A. Katz, and R. R. Alfano, IEEE J. Quantum Electron. **19,** 1477 (1983).
4. M. L. Shand and S. T. Lai, IEEE J. Quantum Electron. **20,** 105 (1984).
5. R. R. Alfano and J. M. Buchert, *Chromium-doped beryllium aluminum silicate laser systems* U.S. Patent 4464761 (1084).
6. S. T. Lai, J. Opt. Soc. Am. B **4,** 1286 (1987).
7. S. N. Barilo, G. L. Bychkov, L. A. Kurnevich, N. I. Leonuk, V. P. Mikhailov, S. V. Shiryaev, V. T. Koyava, and T. V. Smirnova, J. Cryst. Growth **198/199,** 716 (1999).
8. Z. Chen, G. Zhang, H. Shen, and C. Huang, J. Cryst. Growth **244,** 339 (2002).
9. Z. Chen, J. Zeng, W. Zhong, and H. Shen, J. Synth. Cryst. (in Chinese) **31,** 34 (2002).
10. Z. Chen, G. Zhang, C. Huang, and H. Shen, J. Inorganic Mater. (in Chinese) **17,** 1129 (2002).
11. Z. Chen, H. Shen, G. Zhang, and C. Huang, Acta Photon. Sin. (in Chinese) **33,** 382 (2004).
12. U. Fano, Phys. Rev. A **124,** 1866 (1961).
13. Z. Chen, G. Zhang, H. Shen, C. Huang, W. Liu, and L. Huang, Chin. J. Lasers (in Chinese) **30,** 843 (2003).